

## Improving power conversion efficiency in bulk heterojunction P3HT: PCBM organic solar cells by utilizing RGO-TiO<sub>2</sub>

Iman Farjamtalab<sup>1</sup>, AlirezaKashaniniya<sup>1</sup>, Reza Sabbaghi-Nadooshan<sup>1</sup>  
<sup>1</sup>(Department of Electrical Engineering/ Central Tehran Branch, Islamic Azad University, Tehran, Iran)

**Abstract:** In this work we have presented exact optical and physical parameters for P3HT: PCBM solar cells. We have used Langevin model to evaluate recombination rate, utilizing singlet and triplet models for exchange between charge carrier and singlet and triplet excitons. Turning point in our work is to insert RGO-TiO<sub>2</sub> composite layer in bulk heterojunction solar cells. The results indicate that the power conversion efficiency (PCE) can be enhanced in bulk heterojunction P3HT: PCBM solar cells by inserting an interfacial electron transporting layer consisting of reduced graphene oxidetitanium dioxide (RGO-TiO<sub>2</sub>) between the active layer and Al cathode, which improves the PCE of the organic solar cell up to 1.94%.

**Keywords** -Reduced Graphene Oxide(RGO), P3HT:PCBM, power conversion efficiency, organic solar cells.

### I. Introduction

Organic photovoltaic devices have perfect technological potentials to make electrical energy from renewable resources. Furthermore, organic photovoltaic devices have a potential for low cost due to the printing techniques applied to their fabrication [1].

The potential of a flexible, roll-to-roll manufacturing process has made bulk-heterojunction (BHJ) organic solar cells (OSCs) as a promising solution to energy and environmental problems [2-3]. Notwithstanding the benefits of procedure, the power conversion efficiency of OSCs is probably lower in thin-film architectures when compared to high PCE inorganic counterparts. This is fundamentally due to the trade-off between light absorption and exciton diffusion [4-5].

In polymer solar cells, the characteristics such as fill factor (FF), short-circuit current density ( $J_{sc}$ ) and open-circuit voltage ( $V_{oc}$ ) are extremely dependent on the interfacial properties between the electrodes and the active layers [6]. The limitation of diffusion length exciton affects the limitation of charge collection. Hence, the absorption of layers probably requires to be thin enough [4-7].

In recent years, bulk heterojunction OSCs based on P3HT:PCBM active material have received special attention owing to their large absorption [4]. Among the configurations of organic polymer solar cells, graphene or graphene oxide (GO) have been examined as an electrode, an interlayer or an addition to active layer [8].

However, nowadays it is the beginning of incorporating graphene or graphene oxide (GO) into organic polymer solar cells. Graphene, which is mechanically strong, chemically stable, and inert, should improve the durability and simplify the technology of optoelectronic devices. However, the method of graphene synthesis influences on its properties [8]. Graphene is primarily obtained using procedures such as exfoliation, chemical vapour deposition (CVD) and chemical and electrochemical methods [8].

### II. Rgo-Tio2 Analysis In Literature

In the beginning, we want to simulate the results of paper [9] as an evaluation of the model, then we want to present important parameters from valid literature. In the next step, we want to examine the effects of RGO-TiO<sub>2</sub> interfacial layer on power conversion efficiency.

In the paper, there has been represented an organic solar cell with structure ITO/PEDOT:PSS/P3HT:PCBM/Al. The P3HT:PCBM (1:0.8, w/w) solutions were prepared in pure solvent (Dichlorobenzene) and stirred for 48 h under N<sub>2</sub> conditions. First, a 40 nm thick PEDOT:PSS layer was spin coated onto a well-cleaned glass substrate covered with a 100 nm thick layer of indium tin oxide (ITO). Secondly, the photoactive layer was fabricated by depositing the prepared solution via spin coating. The thickness of the photoactive layer was around 120 nm. Finally, the devices were completed by the evaporation of 80 nm Al back electrode at pressure lower than 10<sup>-6</sup> m bar. The result of photoresponse behavior PV devices when illuminated by a UV filtered halogen lamp typical (for these materials in the described device layout with Al cathodes), indicated:  $V_{oc} = 0.39$  V,  $I_{sc} = 8.7$  mA cm<sup>2</sup>, FF = 42% [9]. In this section, we want to analyze the performance of RGO-TiO<sub>2</sub> interfacial layer in organic solar cells. We have presented overall report from the positions of graphene in organic solar cells in the table 1.

**Table 1. Overall report from the positions of graphene in organic solar cells**

structure	$V_{oc}$ (V)	$J_{sc}$ (mA)	FF(%)	PCE	Ref.
ITO/PEDOT:PSS/P3HT:PCBM/Al	0.47	7.86	0.37	1.38	[11]
ITO/GO/P3HT:PCBM/PEDOT:PSS/Al	0.06	0.44	0.07	0.002	[11]
ITO/GO/P3HT:PCBM/GO/Al	0.04	0.68	0.16	0.004	[11]
ITO/PEDOT:PSS/P3HT:PCBM/GO/Al	0.39	4.00	0.3	0.47	[11]
ITO/PEDOT:PSS/P3HT:PCBM/X/Al					
ITO/PEDOT:PSS/P:PC70BM/RGO-TiO <sub>2</sub> /Al	0.76	10.95	0.64	5.33	[11]
ITO/PEDOT:PSS/P3HT:graphene:MDMO-PPV/LiF/Al				1.5	[13]
ITO/ZnO/P3HT:PCBM/graphene oxide (GO) /graphene (for 10 layers of graphene) (for shining from ITO side)	-	-	-	1.88	[14]
	-	-	-	2.5	[14]
ITO/ZnO/P3HT:PCBM/PEDOT:PSS/graphene	-	-	-	3.04	[14]
ITO/GO/P3HT:PCBM/Al	-	-	-	3.5	[15]
ITO/GO/NiOx/P3HT:PCBM/LiF/Al	-	-	-	3.48	[16]
ITO/r-GO/P3HT:PCBM/Ca/Al	-	-	-	3.70	[17]

According to the table1, we can understand the best position for graphene. Reduced graphene oxide-titanium dioxide (RGO-TiO<sub>2</sub>) has been applied to interfacial layers above of the cathode. We are going to investigate the reasons of increase in performance solar cells, including RGO-TiO<sub>2</sub> interfacial layers on the top of cathode. In addition, we will analyze the results of inserting RGO-TiO<sub>2</sub> interfacial layers that have been reported in the paper[12].

In paper [12], the TiO<sub>2</sub> or RGO-TiO<sub>2</sub> was deposited onto the top of P:PC70BM active layer by spin coating method using ethanol as solvent and dried for 1 h before the deposition of Al electrode. The thickness of the TiO<sub>2</sub> or RGO-TiO<sub>2</sub> was about 25–30 nm[12].

The  $J_{sc}$  of the BHJ organic solar cell depends on the light absorption characteristics of the active layer, the exciton dissociation rate and the charge collection/extraction efficiency by the electrodes. The light absorption efficiency is related to the absorption spectral response of the active layer used in the device with and without interfacial layers have been illustrated in Fig.1(C). It can be seen from this figure that the incorporation of the interfacial layer increases the absorption in the whole absorption region. The increased absorption of the active layer with the insertion of the interfacial layer may be one of the reasons of enhancement in the  $J_{sc}$  of polymer solar cells[12].

According to Fig.1(B), the enhancement of optical electric field amplitude for the RGO-TiO<sub>2</sub> interfacial layer is more than the TiO<sub>2</sub> interfacial layer and without interfacial layer. The increasing optical electric field affects increasing photocurrent and  $J_{sc}$  and PCE in the organic solar cells [12].

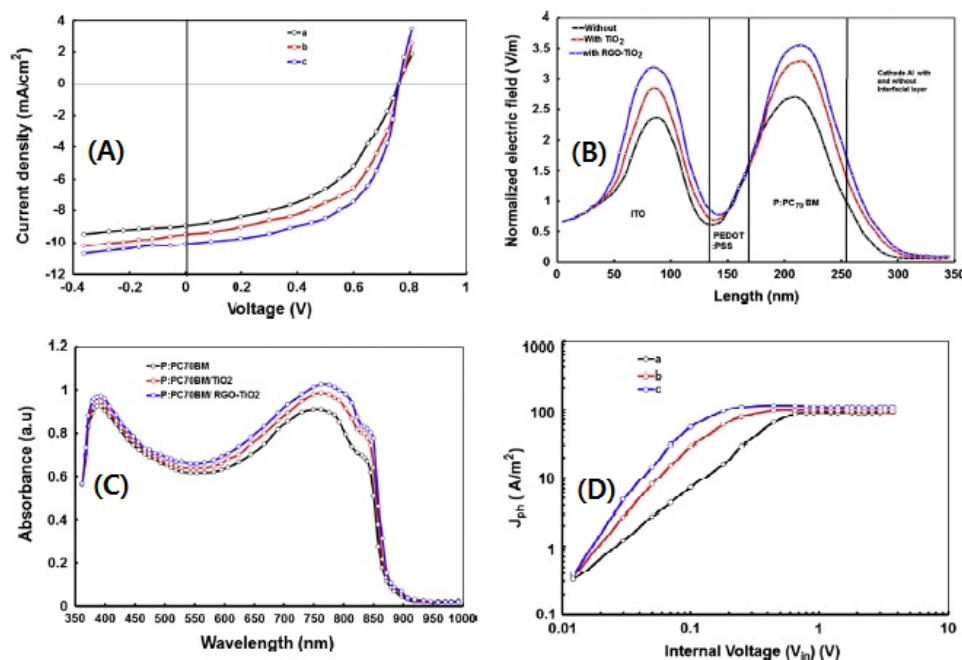


**Fig.1.** (A) Current–voltage characteristics of P: PC70BM solar cells (a) without, (b) with TiO<sub>2</sub> layer and (c) with RGO-TiO<sub>2</sub> composite layer. (B) Distribution of the normalized optical electric field for light inside BHJ devices at the wavelength 745 nm (C) Absorption spectra of active layers with and without interfacial layer. (D) Photocurrent density ( $J_{ph}$ ) for the cells (a) without (a) with TiO<sub>2</sub> layer and (c) RGO-TiO<sub>2</sub> layer [12].

On the other hand, the hole mobility of P:PC70BM is two order of magnitude lower than its electron mobility [18].The imbalance in charge carriers mobility leads to build up of charges in the active layer and affects increasing the charge recombination, which was resulted in a low FF and  $J_{sc}$ .According the electron mobility for the RGO–TiO<sub>2</sub>layer is lower than the TiO<sub>2</sub>layer,the reducing electron mobility affectsreducing the ratio of electron to hole mobility, which consider benefit for achieving a balance charge management/extraction[19]. This balance charge extraction affects increasingFF and  $J_{sc}$  [12].

### III. Model

We utilized Bimolecular Langevin Recombination Model in order to determine recombination rate. The Langevin recombination rate coefficienthas been given in literature [20][21]by equation:

$$r_L(x, y, t) = \frac{q}{\epsilon \epsilon_0} (\mu_n(E) + \mu_p(E)) \quad (1)$$

Where  $\mu_n$ and  $\mu_p$ are electron and hole mobility respectively .The electron-to-hole mobility ratio  $\beta$  is defined by:

$$\beta = \frac{\mu_n}{\mu_p} \quad (2)$$

The Langevin recombination rate is given by:

$$R_{L,n,p}(x, y, t) = r_L(x, y, t)(np - n_i^2) \quad (3)$$

Where n is electron density, p is hole density and  $n_i$  is the intrinsic concentration[10]. The Langevin recombination rate is included in recombination terms in the carrier continuity equations (equations 4 and 5).

The continuity equations for electrons and holes are defined by equations:

$$\frac{\partial n}{\partial t} = \frac{1}{q} \text{div } \vec{J}_n + G_n - R_n \quad (4)$$

$$\frac{\partial p}{\partial t} = \frac{1}{q} \text{div } \vec{J}_p + G_p - R_p \quad (5)$$

Where n and p are the electron and hole concentration,  $\vec{J}_n$ and  $\vec{J}_p$  are the electron and hole current densities,  $G_n$  and  $G_p$ are the generation rates for electrons and holes,  $R_n$  and  $R_p$  are the recombination rates for electrons and holes, and q is the magnitude of the charge on an electron.

furthermore, we used singlet and triplet model for exchange between charged carrier and singlet and triplet excitons (with SILVACO Atlas).Of course we can self-consistently solve the singlet and triplet exciton continuity equations along with the electron and hole drift diffusion equations that have been given by [33] and [34].Almost, ray tracing based on geometrical optic principles has been utilized in order to simulate optoelectronic devices. But in this case, we used Beam Propagation Method (with SILVACO Atlas) [22].Because we need a method that takes into account the wave nature of light. The BPM in LUMINOUS, has been extended to solve a more general Helmholtz Wave Equation (Equation 6).

$$\nabla^2 E(r, t) - \frac{n^2}{c^2} \frac{\partial^2 E(r, t)}{\partial t^2} = 0 \quad (6)$$

Here, E is the electric field of an optical wave, n is the complex refractive index of the material, and c is the speed of light in vacuum.We need to know almost all the physical parameters of each layer in the organic solar cell in order to simulateparameters such as hole and electron mobility, band gap energy, density of state, LUMO and HOMO, dielectric constant. We reportedthese parameters in the table2,3 and 4.

**Table2. Parameter of PEDOT: PSS [23]**

material	Band gap (ev)	HOMO (ev)	LUMO (ev)	permittivity	Refractive index	density of states(ev)	Hole mobility ( $10^{-7} \text{ m}^2 \text{ V}^{-1} \text{ s}^{-1}$ )	Electron mobility ( $10^{-7} \text{ m}^2 \text{ V}^{-1} \text{ s}^{-1}$ )	density of transport sites ( $10^{26} \text{ m}^{-3}$ )
PEDOT:PSS	2.9	5	2.2	3.2	2.1	0.13	1.4	1.4	6

The P3HT has HOMO level at 5.2 ev and LUMO level at 3.3 ev, while for PCBM has been reported: HOMO 6.1 ev and LUMO 4.1 ev. The PEDOT:PSS interlayerhas HOMO at 5.0ev and LUMO at about 2.2 ev [24,25,26,27, 28].

**Table3. Parameter of P3HT: PCBM [9][29]**

material	permittivity	Acceptor doping density ( $N_C$ )( $\text{cm}^{-3}$ )	Dielectric constant	density of transport sites( $N_A$ ) ( $10^{16} \text{cm}^{-3}$ )
P3HT: PCBM	3	$10^{21}$	3	5

We utilized ITO as an anode in solar cells .The characteristics of ITO has been shown in table 4.

**Table4.Parameter of ITO [30]**

material	Band gap (ev)	carrier concentration ( $10^{20}$ )	Refractive index	Electron mobility ( $\text{cm}^2 \text{V}^{-1} \text{s}^{-1}$ )	dielectric constant
ITO	3.8-4.3	2- 7.5	2.2	180	4.1 – 3.3

The final schematicstructure of this work has been shown in Fig.2.

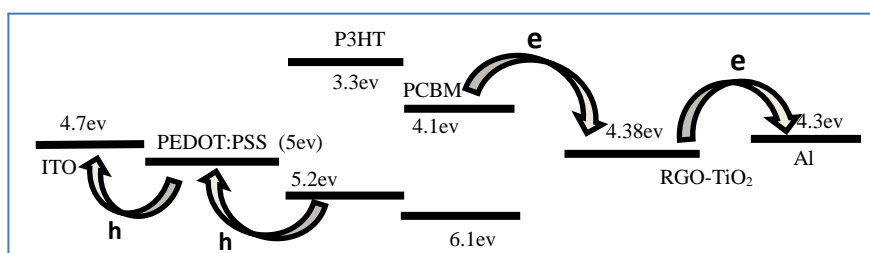


**Fig.2.** Schematic representation of the energy levels (energies given in eV) of the electron donating and electron accepting materials

#### IV. Result And Discussion

AS a primary simulation, we have simulated the structure ITO/PEDOT:PSS /P3HT:PCBM/Al that current–voltage characteristics are in good agreement with the results of paper[9].

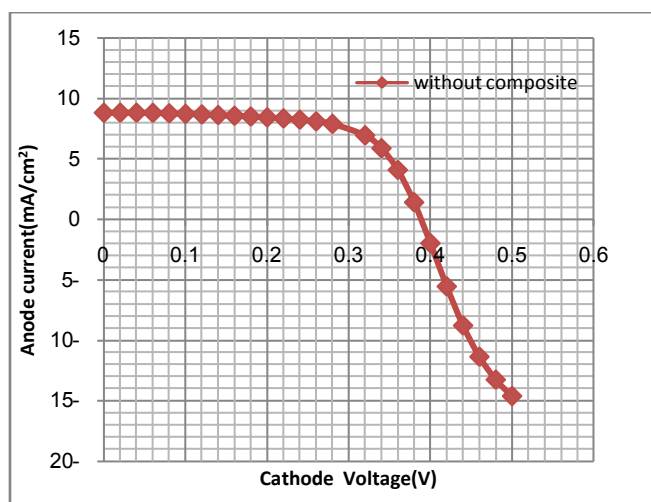


**Fig.3.**Current–voltage characteristics of solar cells with configuration ITO/PEDOT:PSS/P3HT:PCBM /Al

You can see in Fig. 3, the short circuit current and the open circuit voltage are Approximately  $8.7 \text{ mA cm}^{-2}$  and  $3.9 \text{ V}$  respectively. In the second simulation, we want to simulate the configuration ITO/PEDOT:PSS/P3HT:PCBM/ RGO-TiO<sub>2</sub>/Al (see Fig.4); then we will analyze the influence of RGO-TiO<sub>2</sub> (the analysis of RGO-TiO<sub>2</sub> has been described in previous section) on  $J_{sc}$ , FF and PCE through considering the influences of enhancement in the optical absorption and the generation rate of interfacial layer.

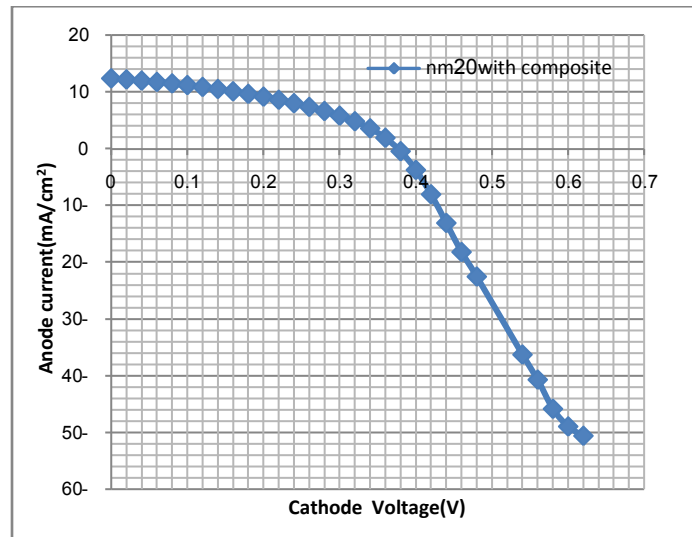


**Fig.4** Current–voltage characteristics of P3HT:PCBM solar cells with RGO–TiO<sub>2</sub> composite layer.

The current–voltage trend of figure 4 is almost like figure 3, but short circuit current has been increased to 12.45 mA/cm<sup>2</sup>. In addition, we investigated and illustrated current–voltage characteristics with different thickness composite layer in Fig.5. According to Fig.5, voltage cathode and anode current have been declined with increasing the thickness of the composite layer. May be, the limitation of diffusion and life time charge carrier are more important reasons for the decline.

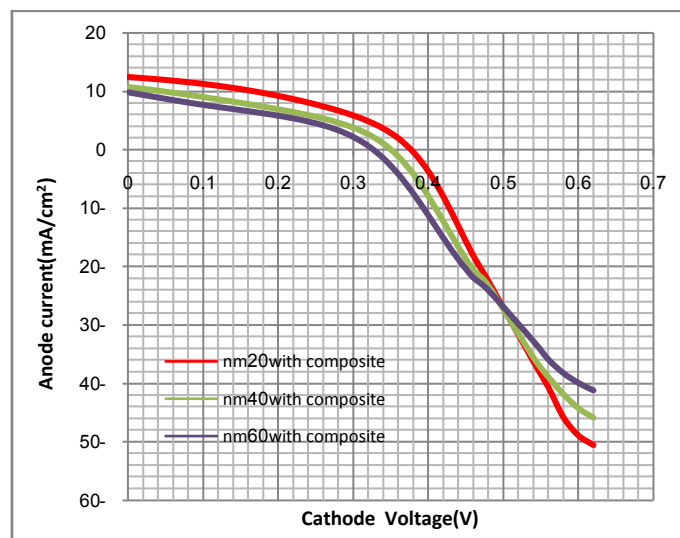


**Fig.5.** Current–voltage characteristics with different thickness composite layer

In addition, we know relation between the current density and the voltage in dark for electron that given by the Mott-Gurney equation (Eq.7) [32]. Where  $\epsilon_r$  is the relative permittivity of the active layer,  $\epsilon_0$  is the permittivity of free space,  $V$  is the applied voltage to the device,  $V_{bi}$  is the built in potential,  $L$  is the device thickness, and  $\mu$  is the electron mobility.

$$J = \left(\frac{9}{8}\right) \epsilon_r \epsilon_0 \mu \frac{(V - V_{bi})}{L^3} \quad (7)$$

In addition to equation 7, we know current density and anode current associate to charge mobility generally. On the other hand, we know mobility depends on temperature. Therefore, we can see the influence of temperature changes on current-voltage curve in Fig.5.

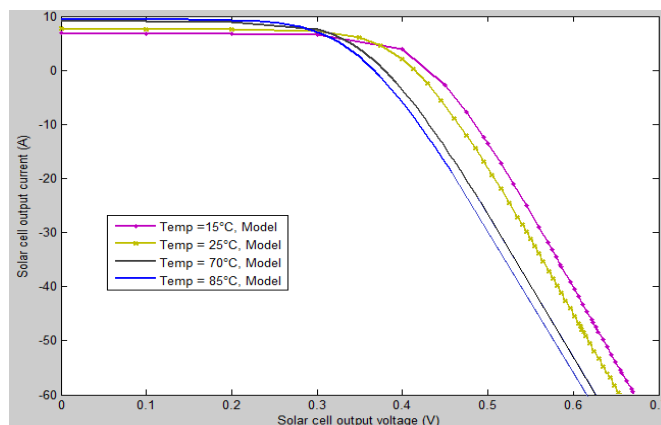


Fig.5. J(V) curve illustrated as a temperature-dependent parameter.

According to explanation above, it seems RGO-TiO<sub>2</sub> interfacial layer is suitable for configuration mentioned include P3HT: PCBM due to the hole mobility magnitude of P3HT:PCBM is lower than the electron mobility. In other words, inserting RGO-TiO<sub>2</sub> interfacial layer causes an optimization of the  $\beta$  parameter (that has been mentioned in the equation 2) and reducing the ratio of electron to hole mobility, which is considered beneficial for achieving a balance charge management. The photovoltaic parameters of P3HT:PCBM solar cells without and with RGO-TiO<sub>2</sub> composite layer have been illustrated in Fig. 6 and table 5.

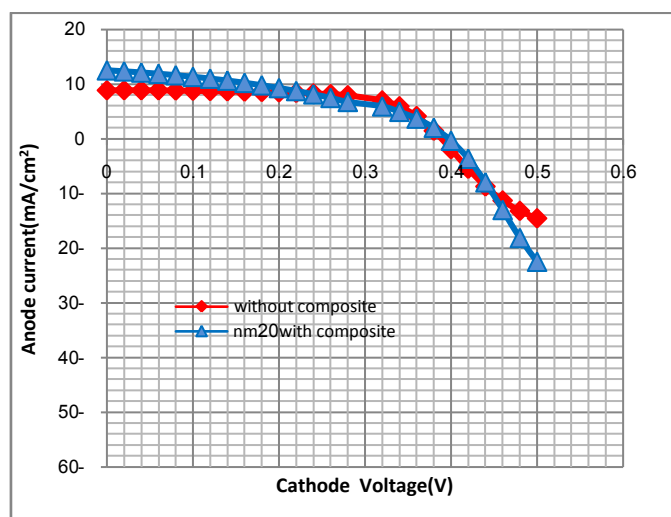


Fig.6. Current-voltage characteristics of P3HT:PCBM solar cells (Cell1) without, (cell2) with RGO-TiO<sub>2</sub> composite layer.

Table 5. Photovoltaic parameters of P3HT:PCBM solar cells without and with RGO-TiO<sub>2</sub> layers.

Device	J <sub>sc</sub> (mA)	V <sub>oc</sub> (V)	PCE(%)
Without interfacial layer[31]	8.7	0.39	1.42
RGO-TiO <sub>2</sub>	12.45	0.39	1.94

### V. Conclusion

We have used RGO-TiO<sub>2</sub> composite, inserted between BHJ active layer consisting of P3HT as donor and PCBM as acceptor and Al cathode electrode. We have compared PCE of the solar cells without and with RGO-TiO<sub>2</sub> interfacial layer. The results indicate overall PCE about 1.42% and 1.94% for solar cells with and without RGO-TiO<sub>2</sub> interfacial layer respectively. Enhancement in J<sub>sc</sub> and FF was resulted in PCE with the incorporation of interfacial layer. The increase in these two parameters was a key feature to the increase in charge generation rate, upon the insertion of the interfacial layer. In addition, we have improved the charge collection through reducing ratio between the electron and hole mobility as a result, reduction in the charge recombination.

## References

- [1]. O. Ourahmoun and M.S Belkaïd, Dependence of the characteristics of organic solar cells on cathode polymer interface, *Revue des Energies Renouvelables*, 2010, 583 – 590.
- [2]. G. Yu, J. Gao, J. C. Hummelen, F. Wudl, A. J. Heeger, *Polymer Photovoltaic Cells: Enhanced Efficiencies via a Network of Internal Donor-Acceptor Heterojunctions*, *Science* 1995, 270, 1789.
- [3]. R. Søndergaard, M. Helgesen, M. Jørgensen, F. C. Krebs, *Fabrication of Polymer Solar Cells Using Aqueous Processing for AllLayers Including the Metal Back Electrode*, *Advanced Energy Materials* 2011, 1, 68.
- [4]. P. A. Troshin, H. Hoppe, J. Renz, M. Egginger, J. Y. Mayorova, A. E. Goryachev, A. S. Peregodov, R. N. Lyubovskaya, G. Gobsch, N. S. Sariciftci, and V. F. Razumov, *Material solubility-photovoltaic performance relationship in the design of novel fullerene derivatives for bulk heterojunction solar cells*, *Adv. Funct. Mater.* 19(5), 779–788 (2009).
- [5]. D. Duche, E. Drouard, J. Simon, L. Escoubas, P. Torchio, J. L. Rouzo, and S. Vedraïne, *Light harvesting in organic solar cells*, *Sol. Energy Mater. Sol. Cells* 95(1), 18–25 (2011).
- [6]. Hong Ma, Hin-Lap Yip, Fei Huang, and Alex K.-Y. Jen, *Interface Engineering for Organic Electronics*, *Adv. Funct. Mater.* 2010, 20, 1371.
- [7]. H. Shen, P. Bienstman, and B. Maes, *Plasmonic absorption enhancement in organic solar cells with thin active layers*, *J. Appl. Phys.* 106(7), 073109 (2009).
- [8]. A. Iwan, A. Chuchmala, *Perspectives of applied graphene: Polymer solar cells*, *Progress in Polymer Science* 37 (2012) 1805–1828
- [9]. Juan Bisquert, Germà Garcia-Belmonte, Antoni Munar, Michele Sessolo, Alejandra Soriano, Henk J. Bolink, *Band unpinning and photovoltaic model for P3HT:PCBM organic bulk heterojunctions under illumination*, *Chemical Physics Letters* 465, 2008, 57–62
- [10]. C. Min, J. Li, G. Veronis, J. Lee, S. Fan, and P. Peumans, *Enhancement of optical absorption in thin-film organic solar cells through the excitation of plasmonic modes in metallic gratings*, *Appl. Phys. Lett.* 96(13), 133302 (2010).
- [11]. A. Chuchmala, M. Palewicz, A. Sikora, A. Iwan, *Influence of graphene oxide interlayer on PCE value of polymer solar cells*, *Synthetic Metals* 169 (2013) 33–40.
- [12]. G.D. Sharma, M.L. Keshtov, A.R. Khokhlov, D. Tasis, C. Galiotis, *Improved power conversion efficiency by insertion of RGO–TiO<sub>2</sub> composite layer as optical spacer in polymer bulk heterojunction solar cells*, *Organic Electronics* 15 (2014) 348–355
- [13]. J. Wang, Y. Wang, D. He, Z. Liu, H. Wu, H. Wang, P. Zhou, M. Fu, *Solar Energy Materials and Solar Cells* 96 (2012) 58–65.
- [14]. Z. Liu, J. Li, Z.H. Sun, G. Tai, S.P. Lau, F. Yan, *The application of highly doped single-layer graphene as the top electrodes of semitransparent organic solar cells*, *ACS Nano* 6 (2012) 810–818.
- [15]. S.S. Li, K.H. Tu, C.C. Lin, C.W. Chen, M. Chowalla, *Solution-processable graphene oxide as an efficient hole transport layer in polymer solar cells*, *ACS Nano* 4 (2010) 3169–3174.
- [16]. M.S. Ryu, J. Jang, *Effect of solution processed graphene oxide/nickel oxide bi-layer on cell performance of bulk-heterojunction organic photovoltaic*, *Solar Energy Materials and Solar Cells* 95 (2011) 2893–2896.
- [17]. J.M. Yun, J.S. Yeo, J. Kim, H.G. Jeong, D.Y. Kim, Y.J. Noh, S.S. Kim, B.C. Ku, S.I. Na, *Solution-processable reduced graphene oxide as a novel alternative to PEDOT:PSS hole transport layers for highly efficient and stable polymer solar cells*, *Advanced Materials* 23 (2011) 4923–4928.
- [18]. M.L. Keshtov, D.V. Marochkin, V.S. Kochurov, A.R. Khokhlov, E.N. Koukaras, G.D. Sharma, *Synthesis and characterization of a low band gap quinoxaline based D-A copolymer and its application as donor for bulk heterojunction solar cells*, *Polym. Chem.* 4 (2013) 4033–4044.
- [19]. K.D.G. Imalka Jayawardena, R. Rhodes, K.K. Gandhi, M.R. Ranga Prabhath, G. Dinesha M.R. Dabera, M.J. Beliatis, L.J. Rozanski, S.J. Henley, S. Ravi, P. Silva, *Solution processed reduced graphene oxide/ metaloxide hybrid electron transport layers for highly efficient polymer solar cells*, *J. Mater. Chem.* A doi: 10.1039/c3ta11822c.
- [20]. Blom, P.W.M., M.J.M. de Jong, and S. Breedijk, *Temperature Dependent Electron-Hole Recombination in Polymer Light-Emitting Diodes*, *Applied Physics Letters* Vol. 71, No. 7 (August 1997): 930-932.
- [21]. Scott, J.C., S. Karg, and S.A. Carter, *Bipolar Charge and Current Distributions in Organic Light-Emitting Diodes*, *J. Appl. Phys.* Vol. 82, No. 3 (August 1997): 1454-1460.
- [22]. Van Roey, J., J. Van Der Donk, P.E. Lagasse., *Beam-propagation method: analysis and assessment*, *J. Opt. Soc. Am.* Vol. 71, No 7 (1981): 803.
- [23]. S. L. M. van Mensfoort, S. I. E. Vulto, R. A. J. Janssen, and R. Coehoorn, *Hole transport in polyfluorene-based sandwich-type devices: Quantitative analysis of the role of energetic disorder*, *PHYSICAL REVIEW B* 78, 2008.
- [24]. E. Bundgaard, F.C. Krebs, *Low band gap polymers for organic photovoltaics*, *Solar Energy Materials and Solar Cells* 91 (2007) 954–985.
- [25]. N. Blouin, M. Leclerc, *Poly(2,7-carbazole)s: Structure–Property Relationships*, *Accounts of Chemical Research* 41 (2008) 1110–1119.
- [26]. G. Dennler, M.C. Scharber, C.J. Brabec, *Polymer-Fullerene Bulk-Heterojunction Solar Cells*, *Advanced Materials* 21 (2009) 1323–1338.
- [27]. F. Liu, J.M. Nunzi, *Air stable hybrid inverted tandem solar cell design*, *Applied Physics Letters* 99 (2011) 063301-1–063301-3.
- [28]. D.C. Marcano, D.V. Kosynkin, J.M. Berlin, A. Sinitskii, Z. Sun, A. Slesarev, L.B. Alemany, W. Lu, J.M. Tour, *Improved Synthesis of Graphene Oxide*, *ACS Nano* 4 (2010) 4806–4814.
- [29]. Germà Garcia-Belmonte, Pablo P. Boix, Juan Bisquert, Michele Sessolo, Henk J. Bolink, *Simultaneous determination of carrier lifetime and electron density-of-states in P3HT:PCBM organic solar cells under illumination by impedance spectroscopy*, *Solar Energy Materials & Solar Cells* 94 (2010) 366–375
- [30]. Takao Nagatomo, Yukihiko Maruta, Osamu Omoto, *Electrical and optical properties of vacuum-evaporated indium-tin oxide films with high electron mobility*, 1990, 17–25
- [31]. (a) A.C. Arango, L.R. Johnson, V.N. Bliznyuk, Z. Schlesinger, S.A. Carter, H.H. Hörhold, *Efficient titanium oxide/conjugated polymer photovoltaics for solar energy conversion*, *Adv. Mater.* 12 (2000) 1689–1692;
- [32]. (b) M. Thelakkat, C. Schmitz, H.W. Schmidt, *Fully vapor-deposited thin-layer titanium dioxide solar cells*, *Adv. Mater.* 14 (2002) 577–581;
- [33]. (c) P.A. Hal, M.M. Wienk, J.M. Kroon, W.J.H. Verhees, L.H. Loeff, W.J.H. Gennip, P. Jonkheijm, R.A.J. Janssen, *Photo-induced electron transfer and photovoltaic response of a MDMO-PPV:TiO<sub>2</sub> bulk heterojunction*, *Adv. Mater.* 15 (2003) 118–121;
- [34]. (d) J.Y. Kim, S.H. Kim, H.H. Lee, K. Lee, W. Ma, X. Gong, *New architecture for high-efficiency polymer photovoltaic cells using solution-based titanium oxide as an optical spacer*, *Adv. Mater.* 18 (2006) 572–576.
- [35]. Z.H. Zhou, Y. Zhang, J. Seifert, S.D. Collins, C. Luo, G.C. Bazan, T.Q. Nguyen, A.J. Heeger, *High efficiency polymer solar cells enhanced by solvent treatment*, *Adv. Mater.* 25 (2013) 1646–1652.

- [36]. Ruhstaller, B., S.A. Carter, S. Barth, H. Riel, W. Riess, J.C. Scott, Transient and Steady-State Behavior of Space Charges in Multilayer Organic Light-Emitting Diodes, *J. Appl. Phys.* Vol. 89, No. 8 (2001): 4575-4586.
- [37]. Verlaak, S., Cheyns D., Debucquoy M., Arkhipov, V. and Heremans P., Numerical Simulation of Tetracene Light-Emitting Transistors: A Detailed Balance of Exciton Processes, *Applied Physics Letters* Vol. 85, No. 12 (Sep 2004): 2405-2407.